

# Charge exchange in 3–30 keV H<sup>+</sup> scattering off clean and AlF<sub>3</sub>-covered Al(111) surfaces

## II. Theoretical study

J. O. Lugo,<sup>1,\*</sup> E. C. Goldberg,<sup>2</sup> E. A. Sánchez,<sup>1</sup> and O. Grizzi<sup>1</sup><sup>1</sup>*Céntro Atómico Bariloche, CNEA, CONICET, Instituto Balseiro, UNC, 8400 S. C. de Bariloche, Río Negro, Argentina*<sup>2</sup>*Instituto de Desarrollo Tecnológico para la Industria Química (INTEC-CONICET-UNL), and Facultad de Ingeniería Química (UNL), cc91, 3000-Santa Fe, Argentina*

(Received 15 December 2004; revised manuscript received 14 April 2005; published 11 July 2005)

The collision process of H<sup>+</sup> with clean and AlF<sub>3</sub> covered Al(111) surfaces is theoretically studied for large scattering angles and different ion incoming energies. The energy distributions of the charge fractions are analyzed as a function of the backscattered particle energy. Important differences between the two surfaces are found: in the case of pure Al the outgoing hydrogen particles are predominantly neutral, with a 10% of negative ions, while in the case of AlF<sub>3</sub> an important positive charge fraction is observed. The theoretical calculation reproduces the experimental trends, and shows that these results are strongly related with the electronic structures in each case. In both surfaces a resonant mechanism is responsible for the charge exchange, but while in the pure Al case only the valence band states are involved, in the AlF<sub>3</sub> case the promotion of the projectile energy level by the interaction with the core surface states inhibits the electron capture from the valence band.

DOI: [10.1103/PhysRevB.72.035433](https://doi.org/10.1103/PhysRevB.72.035433)

PACS number(s): 79.20.Rf, 34.70.+e, 34.10.+x

### I. INTRODUCTION

Quantitative information about the dynamics of the electron transfer at surfaces can be obtained from experiments in which ionic beams are scattered off the surface and the charge states of the particles are analyzed. The particular case of hydrogen ions scattered off both metallic and insulator surfaces has been widely studied in different scattering conditions. There are experiments that involve: energy distributions of negative and positive charge fractions of hydrogen backscattered from different solid surfaces bombarded by 5–15 keV protons at normal incidence;<sup>1,2</sup> ion scattering spectroscopy or energy loss measurements of backscattered low energy hydrogen ions (100–500 eV) from ionic surfaces (LiCl),<sup>3,4</sup> of 4 keV hydrogen ions from a Mg surface as a function of oxygen exposure;<sup>5</sup> ion fraction measurements for some given scattering configurations with regard to incident and reflected angles (scattering angles of 3.5 and 38°) of 1–4 keV hydrogen ions scattered off metallic (Al), insulator (MgO) and semiconductor surfaces (Si).<sup>6–10</sup> The negative ion formation in small-angle (grazing) scattering from the surface is thoroughly discussed in the review of Borisov *et al.*<sup>11</sup> At metal surfaces negative ion formation proceeds via a resonant charge transfer process between the electronic states of the valence band and the affinity level downward shifted due to the image potential. The increase of the negative ion yield with exit angle<sup>6,7</sup> can be qualitatively related to a larger survival of negative ions for higher perpendicular velocities  $v_{\text{perp}}$  with respect to the surface plane (shorter dwelling times near the surface). However attempts to fit the ion fractions with a simple expression like the one for the free-electronlike metal surfaces  $\exp(-\Gamma v_{\text{perp}})$  (Ref. 12) were not successful.<sup>9</sup> While considering the short- and long-range interactions to define the level shift of the projectile within a quantum dynamical description of the collision,<sup>13</sup> the experimental trends of the ion fraction as a function of the exit angle in the

case of 1, 2, and 4 keV hydrogen scattered from the Al surface<sup>6,7</sup> were well reproduced. The case of wide bandgap insulators is very different from the free electron metal case. The affinity levels of negative ions usually lie either in the band gap or in the conduction band, and the image potential effect reduced in front of a dielectric surface, is expected to be unable to provide a downward shift enough to bring them into resonance with the valence band. Then one could conclude that the negative ion formation is not possible. However it occurs and more efficiently than in metal surfaces in some cases. For grazing exit angles (3.5°) the negative ion yield is quite small for a clean Mg surface, but as the surface is exposed to oxygen the yield increases substantially.<sup>14,10</sup> Ion fraction measurements for grazing scattering of F from Ag(111) exposed to increasing doses of Cl<sub>2</sub> showed initially a decrease in the F<sup>-</sup> ion fraction in submonolayer chemisorption stages and then a sudden increase when AgCl islands start to form, indicating a specific local character of the electron transfer process on the dielectric layer.<sup>5</sup> The increment of the negative ion fraction has been interpreted in terms of an electron loss to the conduction band of the insulator suppressed by the large band gap, and an electron capture in binary collisions at the anion sites.<sup>11</sup> Enhanced H<sup>-</sup> formation was also observed in backscattering from the cation sites (Li<sup>+</sup>) of the surface compared to backscattering from the anion sites (F<sup>-</sup>),<sup>3,4</sup> being found in this case that the short range interactions with the surface atoms determine the mechanism of charge exchange.<sup>15</sup> It is evident that charge exchange processes occurring between atoms and surfaces depend strongly on the scattering conditions, the incoming energy and nature of the atomic projectile, and the electronic structure of the surface.

In this work we studied the ion fractions for 3–30 keV H<sup>+</sup> projectiles scattered off clean and AlF<sub>3</sub> covered Al(111) surfaces, measured at a scattering angle of 108° and for an incident direction of 15° respect to the surface plane.<sup>16,17</sup> The

corresponding time-of-flight (TOF) spectra converted to energy distributions show that the particles leaving the surface are mainly particles that have had multiple collisions in their incoming and outgoing trajectories inside the solid, and consequently they have suffered large energy losses. In the case of clean Al surface the scattered particles are mainly neutral atoms with a small negative ion fraction ( $\sim 12\%$ ), while an important fraction ( $\sim 33\%$ ) of positive ions emitted from the  $\text{AlF}_3$  covered Al surface is found. The point-by-point ion fractions as a function of the outgoing energy calculated from the TOF spectra show little dependence on the incoming energy. We propose a model calculation to describe the quantum dynamical aspects of the charge exchange process occurring along the outgoing trajectory of the projectile, by considering that the initial velocity and charge state are determined by its previous history inside the solid. In this model the interaction between the atom and the surface involves the extended and localized features of the surfaces, and the atom-atom interactions within a mean-field picture. The Al(111) surface is well described through its local density of states,<sup>18</sup> while a cluster model is proposed for the  $\text{AlF}_3$  ionic surface. Different initial charge configurations for the emitted hydrogen are considered depending on the crossing either along metallic or ionic surface layers; and hydrogen level shifts by either the image potential in the case of metallic surface or by the Madelung potential in the ionic surface, have been taken into account.

The theoretical description of the interacting systems and the calculation of the ion fractions are described in Sec. II. In Sec. III the results are discussed, and Sec. IV is devoted to the summarized conclusions.

## II. THEORY

### A. The interaction with clean Al(111) surface

The formalism for describing the resonant neutralization mechanism in  $\text{H}^+$  scattering from an Al surface has been developed in a previous work.<sup>13</sup> The electronic processes involve the interaction with the surface atoms inside a sphere of radius equal to 12 a.u. (neighbor-atom sphere) centered at the projectile position in each point of the trajectory, and a bond-pair model<sup>19</sup> allows us to recover the Anderson-Newns Hamiltonian where the on-site energy and hopping terms are defined up from both the local density of states of the surface and the atomic properties of the one- and two-electron interactions. In this form the level shift of the incoming particle is calculated by considering the short-range interactions well treated by a mean-field approximation, the long-range one through the image potential, and the energy shift due to the atom motion in the surface frame. Both, the extended nature of the surface through the local and partial density of states and the localized atom-atom hopping integrals calculated within a mean-field approximation, define the atom-surface hopping terms.

In the case of  $\text{H}^+$  colliding with an Al surface, the ionization level ( $-13.6$  eV) is resonant with the valence band and a practically total neutralization is expected in the incoming trajectory. Then, the  $\text{H}^-$  formation from neutral atoms provides a good approximation to the  $\text{H}^+/\text{Al}$  collision. Taking

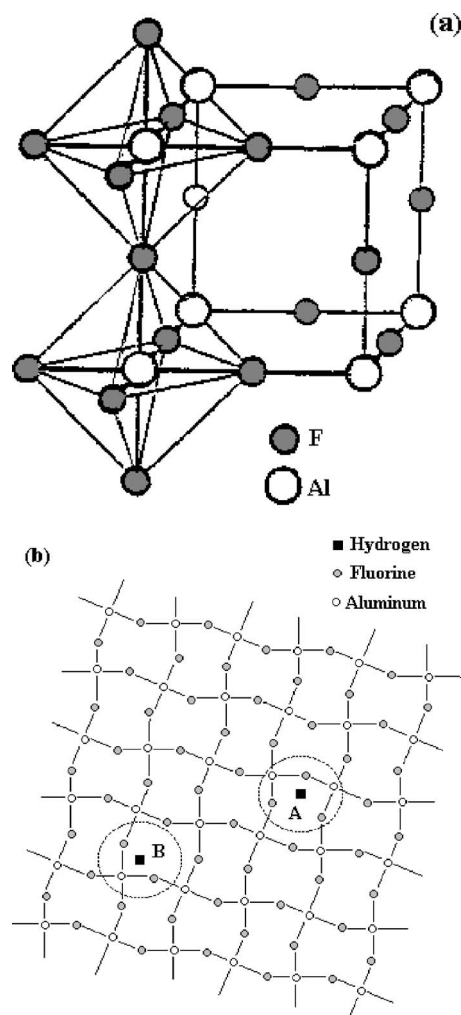


FIG. 1. (a) Crystalline structure of  $\text{AlF}_3$ ; (b) proposed  $\text{AlF}_3$  surface and the two initial (A and B) positions assumed for the outgoing hydrogen.

into account the energy locations of the ionization and affinity levels with respect to the Fermi level, and the neutral H as the incoming particle, small changes of the initial spin-state occupation are expected. Then, freezing the occupation of the first spin state to its initial value ( $\langle n_1 \rangle = 1$ ), and considering only the variations of the average occupation of the second spin-state ( $\langle n_2 \rangle$ ) in the presence of the mean field provided by the first electron, is a rather good approximation to the  $\text{H}^-$  formation in the  $\text{H}/\text{Al}$  collision.<sup>20</sup> This picture leads to a spinless approach of the atom-surface interaction. The same picture was used in this work for the emission case where only the outgoing part of the trajectory is considered. The wide band characteristics of the Al(111) band structure make possible that the positive ions  $\text{H}^+$  formed due to violent collisions along the crossing of the surface layer can be efficiently and rapidly neutralized. Then, the initial neutral charge configuration for the hydrogen atom close to the surface is well justified in this case.

The expression of the spinless approximation to the Hamiltonian is

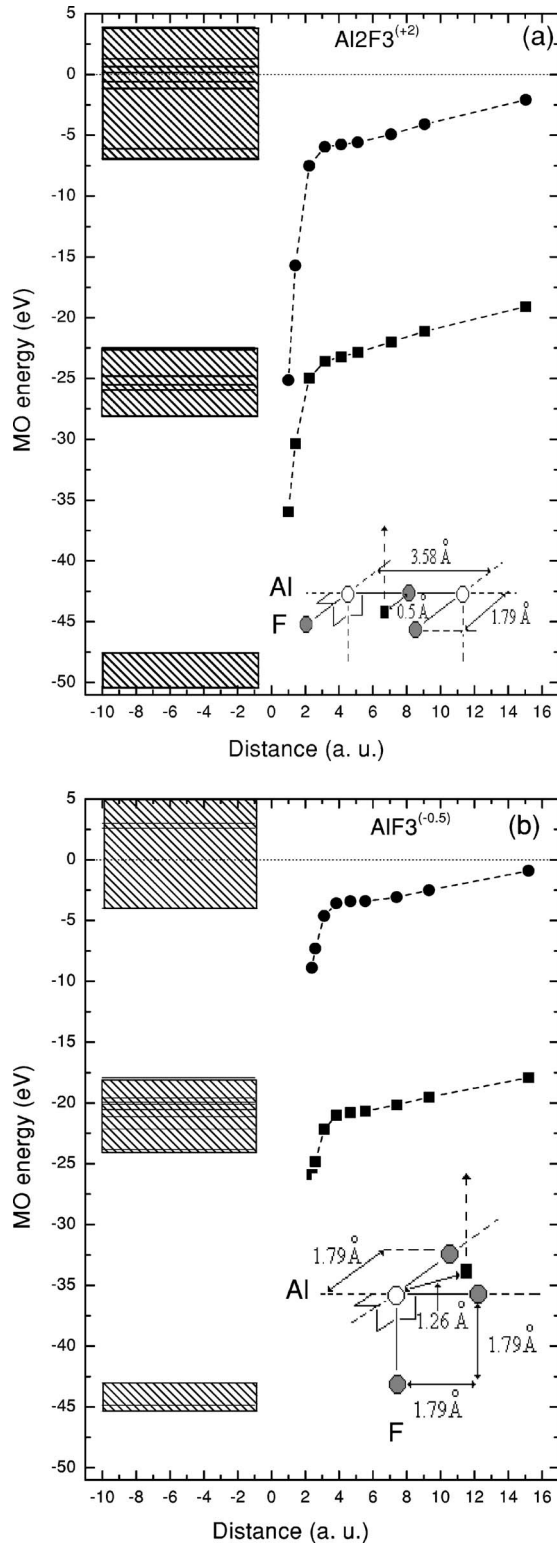


FIG. 2. The electronic band structure suggested from the molecular orbital states, and the ionization (full squares) and affinity (full circles) levels of hydrogen as a function of the distance from the surface for: (a)  $\text{Al}_2\text{F}_3$  clusterlike surface; (b)  $\text{AlF}_3$  clusterlike surface. Both clusters are shown as insets in each case: full circles correspond to F atoms and empty ones to Al; the full square symbol indicates the initial position for the emitted hydrogen. The distances between atoms in both clusters are also indicated.

$$H(t) = \sum_{\mathbf{k}} \varepsilon_{\mathbf{k}} \hat{n}_{\mathbf{k}} + \sum_c \varepsilon_c \hat{n}_c + E_a(t) \hat{n}_a + \sum_{\mathbf{k}} [V_{a\mathbf{k}}(t) \hat{c}_a^+ \hat{c}_{\mathbf{k}} + \text{h.c.}] + \sum_c [V_{ac}(t) \hat{c}_a^+ \hat{c}_c + \text{h.c.}], \quad (1)$$

where the index  $a$  refers to the active state localized on the projectile atom with energy  $E_a(t)$ , while the indexes  $\mathbf{k}$  and  $c$  refer to the valence-band and core-band states of the solid respectively, with energies  $\varepsilon_{\mathbf{k}}$  and  $\varepsilon_c$ ; being  $V_{a\mathbf{k}}(t)$  and  $V_{ac}(t)$  the respective atom-surface hopping terms. The occupation operators are defined as  $\hat{n}_{\mathbf{k}} = \hat{c}_{\mathbf{k}}^+ \hat{c}_{\mathbf{k}}$ ,  $\hat{n}_a = \hat{c}_a^+ \hat{c}_a$ . The time dependence of the parameters comes from the classical trajectory  $\mathbf{R}(t)$  assumed as a linear one with constant velocity  $v$ .

In the spinless approximation  $\langle \hat{n}_a(t) \rangle$  gives the probability that the projectile state is occupied at the time value  $t$ . The other possibility is the empty state with probability given by  $1 - \langle \hat{n}_a(t) \rangle$ . The negative ion fraction  $\Gamma^-$  is then calculated as the occupation  $\langle \hat{n}_a(\infty) \rangle_{H^0 \rightarrow H^-}$  of the initially empty hydrogen affinity level. Under the assumption of independent processes, the positive ion fraction  $\Gamma^+$  can be calculated from the electron loss probability of the initially occupied ground state  $1 - \langle \hat{n}_a(\infty) \rangle_{H^0 \rightarrow H^+}$  by considering in this case the ionization level as the active one,

$$\Gamma^+ = (1 - \langle \hat{n}_a(\infty) \rangle_{H^0 \rightarrow H^-}) * (1 - \langle \hat{n}_a(\infty) \rangle_{H^0 \rightarrow H^+}). \quad (2)$$

This way of calculating  $\Gamma^-$  and  $\Gamma^+$  is a good approximation for a positive ion fraction much smaller than the negative one; otherwise a treatment that contemplates simultaneously both channels, like a time-dependent Hartree-Fock calculation, would be more appropriate.

The average occupation number  $\langle \hat{n}_a(t) \rangle$  was calculated from the following Green function at equal times<sup>21</sup> as:

$$F_{aa}(t, t') = -i \langle \hat{c}_a^+(t') \hat{c}_a(t) - \hat{c}_a(t) \hat{c}_a^+(t') \rangle,$$

$$\langle \hat{n}_a(t) \rangle = (1 - i * F_{aa}(t, t')) / 2.$$

The equations of motion of this Green function and the other necessary one,  $G_{aa}(t, t') = -i \Theta(t' - t) \langle \hat{c}_a^+(t') \hat{c}_a(t) + \hat{c}_a(t) \hat{c}_a^+(t') \rangle$ , introduce self-energies defined in terms of the local density of states of the Al surface and the atomic H-Al hopping integrals.<sup>13</sup>

### B. The interaction with the $\text{AlF}_3$ surface

The  $\text{AlF}_3$  crystalline solid corresponds to a rhombohedral structure  $\text{MF}_6$  such as the one shown in Fig. 1(a).<sup>22</sup> The distances between atoms are 2.542 Å for F-F and 1.797 Å for Al-F; being the F-Al-F angle of  $90^\circ$  and the Al-F-Al angle of  $157.07^\circ$ . To our knowledge, the composition and the crystallography of thin film  $\text{AlF}_3$  surfaces is not known. Our experimental results<sup>16,17</sup> indicated that the film grown at room temperature completely covers the substrate presenting no long range crystallographic order and good  $\text{AlF}_3$  insulator properties. This film would be stoichiometric, but terminated with two F atoms per Al one. All these observations lead to the proposal for the  $\text{AlF}_3$  surface shown in Fig. 1(b) where distances and relative orientations among Al and F atoms are

the same as in the crystalline solid. In this kind of surface construction the Al atoms in the surface layer have a charge of (+2.5), while (+3) is the charge of bulk Al atoms. The F atom charge is (−1), being accomplished in this form the charge neutrality of the surface.

The two possible initial positions *A* and *B* indicated in Fig. 1(b) were considered for the hydrogen going out from the surface. The interaction was calculated by considering the clusters  $\text{Al}_2\text{F}_3^{(+2)}$  in the case *A*, and  $\text{AlF}_3^{(-0.5)}$  in the case *B*, which involve the nearest target atoms within a sphere of radius of  $\sim 4.5$  Å centered at the initial position of hydrogen [see the insets in Figs. 2(a) and 2(b)]. Both clusters were embedded in the residual point-charge field of the  $\text{AlF}_3$  semicrystal accordingly with Fig. 1(b) in order to account for the Madelung potential. It is shown in Figs. 2(a) and 2(b) the molecular orbitals (MO) obtained from a full electron self-consistent Hartree-Fock calculation.<sup>23</sup> They suggest the  $\text{AlF}_3$  surface band structure with a band gap of  $\sim 15$  eV, a valence band width of  $\sim 6$  eV and a positive affinity (the bottom of the conduction band is below the vacuum level). The valence band is mainly of F-2*p* nature, while the conduction band is formed by Al-3*s* and Al-3*p* orbitals. The core states F-2*s* appear as a narrow band around −49 eV, and the F-1*s* and Al-2*s* around −714.3 and −142.8 eV, respectively.

### 1. A model for the atom-surface interaction

The projectile-cluster interacting system was assumed as a “giant dimeric system” with the isolated cluster described in terms of its own eigenstates ( $\Phi_K$ ), and the interaction described by the bond-pair model Hamiltonian<sup>24</sup>

$$H = \sum_{\sigma} \epsilon_{a\sigma}(R) \hat{n}_{a\sigma} + \sum_{K,\sigma} \epsilon_{K\sigma}(R) \hat{n}_{K\sigma} + \sum_{\alpha,\sigma} (V_{aK,\sigma}(R) \hat{c}_{a\sigma}^{\dagger} \hat{c}_{K\sigma} + \text{h.c.}) + V_{n-n}, \quad (3)$$

where the different Hamiltonian terms are written in the symmetrically orthogonalized  $\{\Phi_K, \Phi_a\}$  basis set. A mean field approximation on the two-electron interactions was performed. This model Hamiltonian has been used for the calculation of several dimers within a full electron unrestricted Hartree-Fock (HF) approximation, leading to very satisfactory results concerning binding energies, equilibrium distances, and vibration frequencies.<sup>24,25</sup> The one-electron integrals involved in the Hamiltonian terms include the electron interaction with the nuclei of the cluster atoms and with the residual point-charge field of the  $\text{AlF}_3$  semicrystal. While  $V_{n-n}$  accounts for the projectile nucleus interaction with the nuclei of the  $\text{Al}_x\text{F}_y$  cluster as well as with the point-charge field of the ionic surface.

The hopping parameters  $V_{aK}(R)$ , where the subscripts *a* and *K* denote the orthogonalized states that asymptotically tend to the atomic state of the projectile and the MO of the isolated cluster, respectively, were obtained from the total energy calculation ( $E^+(R)$  in the case of a positive ion) of the projectile interacting with the clusterlike surface without allowing charge-transfer between them. The total energy of the neutral projectile interacting with the surface ( $E^0(R)$ ) was calculated similarly, and the ionization energy of the projec-

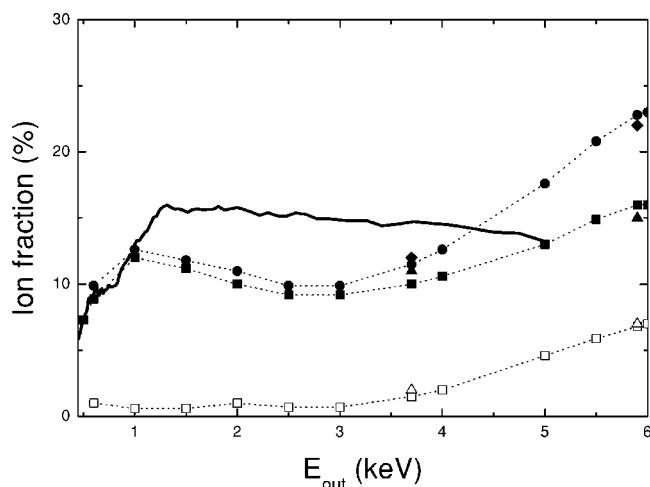


FIG. 3. Ion fractions for hydrogen atoms going out from a clean Al surface as a function of the outgoing energy: empty square symbols indicate the positive fraction ( $\Gamma^+$ ), full squares the negative fraction ( $\Gamma^-$ ), and full circles the total fraction ( $\Gamma$ ). The solid line corresponds to the experimental data averaged over different incoming energies. The ion fractions calculated for single scattering collisions (SS) and for two incoming energies, 4 and 6.5 keV, are also shown: empty triangles are used for  $\Gamma^+$ , full triangles for  $\Gamma^-$ , and full diamonds for  $\Gamma$ .

tile atom was obtained from the difference  $E^0 - E^+$ . In the same way, by calculating the total energy for the negative ion case ( $E^-(R)$ ), the affinity level was calculated as ( $E^- - E^0$ ). In Fig. 2 the ionization ( $\epsilon_I$ ) and the affinity ( $\epsilon_A$ ) levels as a function of the projectile-target distance are shown for each cluster (in the  $\text{Al}_2\text{F}_3$  clusterlike surface the distance is measured respect to the F atom between the two Al ones, while in the  $\text{AlF}_3$  case the origin is at the Al atom). Significant level shifts ( $\sim 2-3$  eV) at large distances produced by the Madelung potential are found. The ionisation level of a free H is placed in front of the aluminum fluoride gap, but it can be resonant with the valence band for distances *R* from the surface in a range of 2–16 a.u. because of the level shifting caused by the Madelung potential (Fig. 2). The process of resonant neutralization should be less efficient in  $\text{AlF}_3$  than in  $\text{Al}(111)$  because of the difference in electron mobility, much faster in the metallic surface than in the insulator, and the different times spent in front of the valence band. The hole lifetime is  $\hbar/W$  with *W* the valence bandwidth. For the case of the calculated clusters *W* is about 5.7 eV, while for Al is 11.5 eV. This produces an increase of the positive ion fraction for  $\text{AlF}_3$  (less neutralization) when compared with  $\text{Al}(111)$ .

The H affinity level is placed in front of the aluminum fluoride cluster gap for distances lower than 2 a.u., and in front of the empty conduction band for  $d > 2$  a.u. If the negative state has not been occupied when the hydrogen atom leaves the surface, the probability to capture electrons from the insulator surface will be negligible.

### 2. The time-dependent process along the outgoing trajectory

In the case of an ionic surface, the neutralization of the  $\text{H}^+$  ions formed due to violent collisions occurring during the

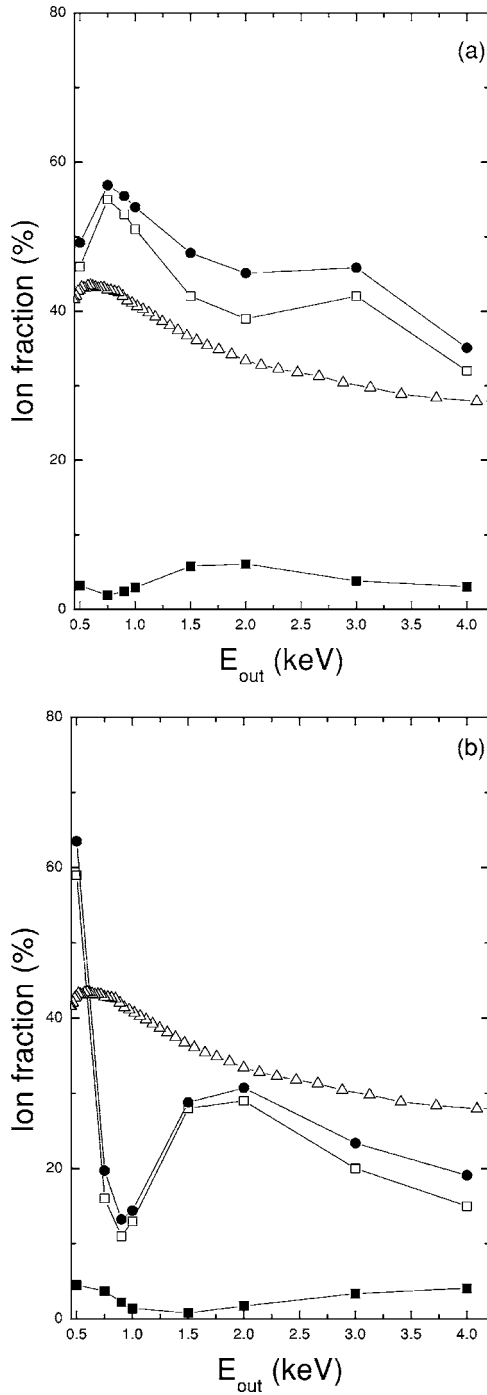


FIG. 4. Ion fractions for  $\text{H}^+$  going out from an  $\text{AlF}_3$  covered Al surface as a function of the outgoing energy. (a)  $\text{Al}_2\text{F}_3$  clusterlike surface; (b)  $\text{AlF}_3$  clusterlike surface. The negative fraction ( $\Gamma^-$ ) is indicated by full square symbols, the positive fraction ( $\Gamma^+$ ) by empty square symbols, and the total one by full circles. The experimental results averaged over different incoming energies are indicated by empty triangles.

crossing of the surface layer is expected to be largely inhibited because of the large band gap and the relatively narrow valence bandwidth. Then, the initial charge configuration for the outgoing hydrogen was assumed positive in this case. An appropriate treatment taking into account the twofold degen-

erate spin states like the one based on an Anderson Hamiltonian in the infinite correlation approximation, would be desirable, but is out of the scope of this work. Then, as a first attempt to calculate the charge exchange, we used a spinless approach to the electronic part of the Hamiltonian (3) for describing the neutralization of the outgoing  $\text{H}^+$  (electron transfer to the ionization level), and also the negative ion formation from neutral hydrogen (electron transfer to the affinity level),

$$H = \varepsilon_{I(A)}(t)\hat{n}_a + \sum_K \varepsilon_K \hat{n}_K + \sum_K (V_{aK}(t)\hat{c}_a^\dagger \hat{c}_K + \text{h.c.}). \quad (4)$$

In a similar way to the clean Al case, the ion fractions were defined as

$$\Gamma^+ = 1 - \langle \hat{n}_a(\infty) \rangle_{\text{H}^+ \rightarrow \text{H}^0}, \quad (5)$$

$$\Gamma^- = \langle \hat{n}_a(\infty) \rangle_{\text{H}^+ \rightarrow \text{H}^0} * \langle \hat{n}_a(\infty) \rangle_{\text{H}^0 \rightarrow \text{H}^-}. \quad (6)$$

These approximated expressions are expected to describe appropriately the case where the negative fraction is much less than the positive one. The assumption of independent processes is less valid for ionic surfaces where the lifetime of the hole is larger than in the metal surface case. But the majority ion fractions, positive in  $\text{AlF}_3$  and negative in Al, are calculated by taking into account quite properly the effect of different hole lifetimes in both surfaces.

The average occupation number  $\langle \hat{n}_a(t) \rangle$  was obtained from the following time-dependent Green functions:

$$G_{am}(t, t_0) = i\Theta(t - t_0) \langle c_m^+(t_0)c_a(t) + c_a(t)c_m^+(t_0) \rangle,$$

where  $m$  refer to the surface and projectile states  $\{\Phi_K, \Phi_a\}$  that diagonalize the system without interaction, and  $t_0$  corresponds to the initial time value. It is straightforward to see that the average occupation number in the  $a$ -state can be calculated as

$$\langle n_a(t) \rangle = \sum_{M(\text{occupied})} |G_{aM}(t, t_0)|^2, \quad (7)$$

where  $M$  runs over the initially occupied states. The  $G_{am}(t, t_0)$  functions were calculated by solving their equations of motion accordingly to the spinless approximation (4) to the interaction Hamiltonian.<sup>15</sup> The self-energies in this case are defined in terms of the hopping integrals between the hydrogen state and the MO states of the  $\text{Al}_x\text{F}_y$  clusterlike surface.

### III. RESULTS AND DISCUSSION

#### A. Clean Al(111) surface

The negative ion fraction  $\Gamma^- = \langle \hat{n}_a(\infty) \rangle_{\text{H}^0 \rightarrow \text{H}^-}$ , the positive one  $\Gamma^+$  given by the expression (2) and the total ion fraction  $\Gamma^{\text{ion}} = \Gamma^- + \Gamma^+$  are shown in Fig. 3 as a function of the outgoing energy  $E_{\text{out}}$ . In the same figure the measured point-by-point ion fractions<sup>17</sup> averaged over different incident ion energies are included. For outgoing energies lower than 5 keV the experimental trends are reproduced by the calculation, and the calculated values for  $\Gamma^-$  ( $\sim 8$ –11%) and

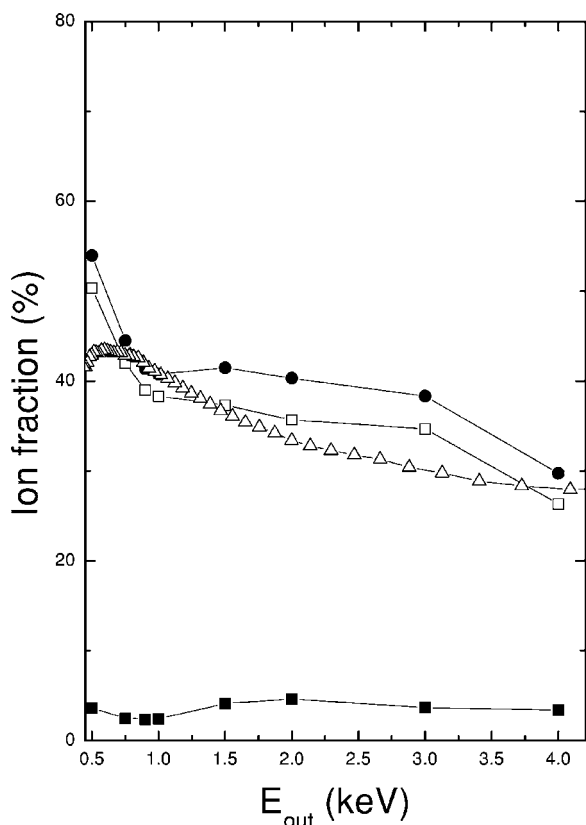


FIG. 5. Averaged ion fractions from the two clusterlike surfaces,  $\text{Al}_2\text{F}_3$  and  $\text{AlF}_3$ , as a function of the outgoing energy:  $\Gamma^+$  (empty squares),  $\Gamma^-$  (full squares), and  $\Gamma$  (full circles). The empty triangles correspond to the averaged experimental result.

$\Gamma^+$  ( $\sim 1-2\%$ ) are in agreement with the measured ones.<sup>17</sup> For larger  $E_{\text{out}}$  the positive ion fraction becomes comparable with the negative one. Taking into account that for these energy values, the ionization and the affinity levels cannot be separated within the uncertainty introduced by the hydrogen velocity ( $\Delta E \sim v > 0.45$  a.u.), a more appropriate calculation than the spinless approximation is required for outgoing energies larger than 5 keV. In Fig. 3 we show the results for  $\Gamma^-$  and  $\Gamma^+$  obtained by assuming a single scattering collision with an incident angle of  $15^\circ$ , for 4 and 6.5 keV incoming energies. The agreement with the results obtained by considering only the outgoing trajectory supports the idea of a complete neutralization close to the surface. We arrive at the same conclusion by observing that the same value of the negative ion fraction is obtained when considering the negative charge as the initial one for the emission process. In all these calculations the core states of Al have been considered, however we found no change in the results when they are eliminated from the dynamical calculation. Then, we can conclude that a resonant mechanism involving only the band states is responsible for the charge transfer process, and that the final state occupation is not affected by the strong hybridizations with the core states occurring at distances very close to the surface.

### B. $\text{AlF}_3$ surface

In Fig. 4(a) the ion fractions calculated for hydrogen going out from the initial position (A) [Fig. 1(b)], which in-

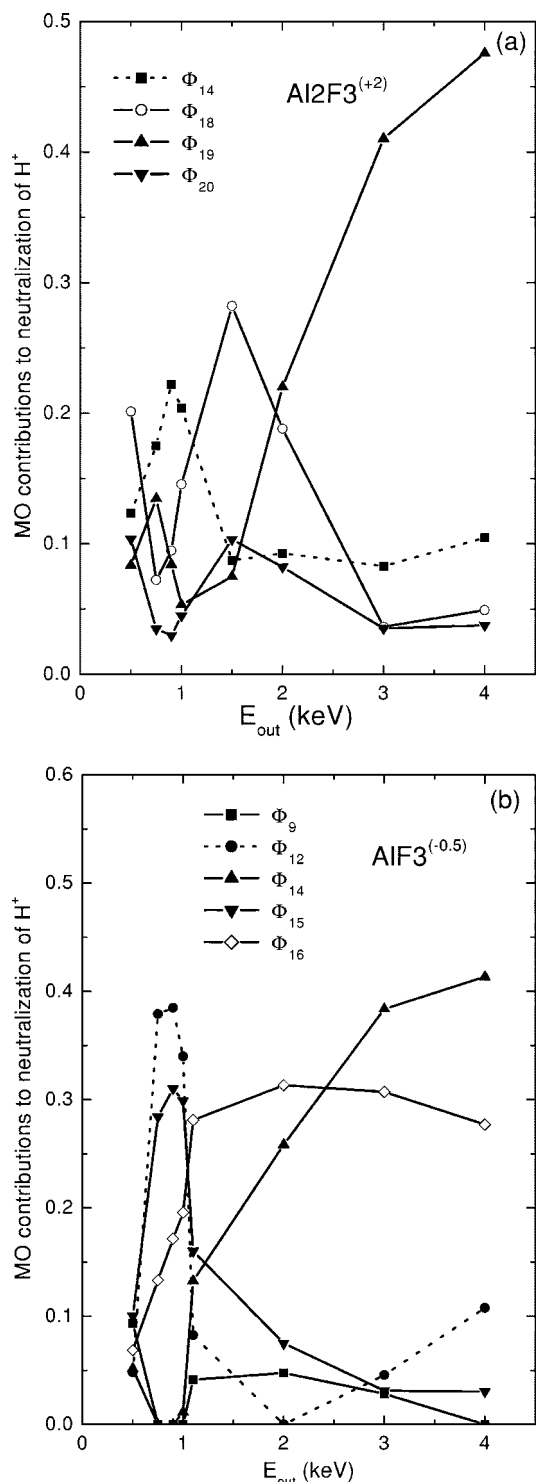


FIG. 6. Contributions of the different MO to the hydrogen state occupation as a function of the outgoing energy  $E_{\text{out}}$ . (a)  $\text{Al}_2\text{F}_3$  clusterlike surface; (b)  $\text{AlF}_3$  clusterlike surface. A full explanation is given in the text.

volves the  $\text{Al}_2\text{F}_3$  clusterlike surface [Fig. 2(a)], are compared with the point-by-point ion fractions<sup>17</sup> measured for the case of  $\text{AlF}_3$  covered  $\text{Al}(111)$  surface and averaged over different incident ion energies. In this figure  $\Gamma^+$ , and  $\Gamma^-$ , given by expressions (5) and (6), respectively, and the total

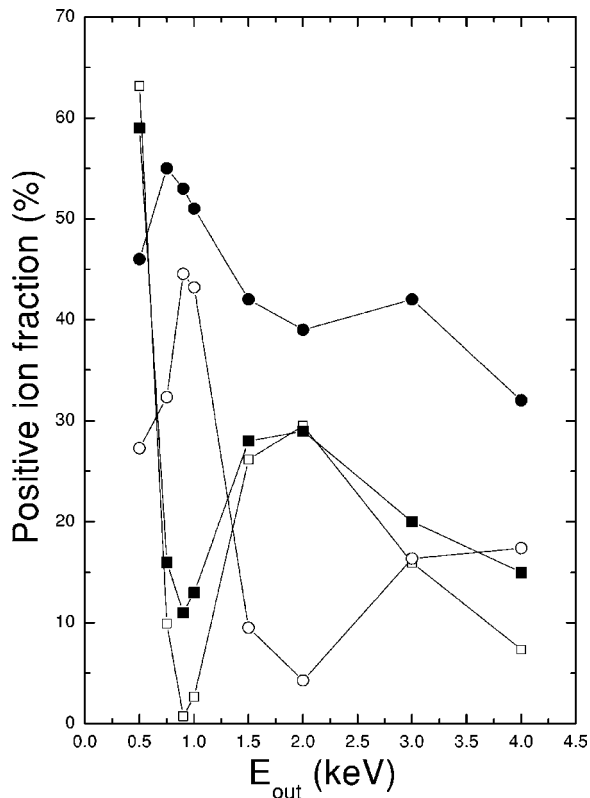


FIG. 7. Positive ion fractions as a function of the outgoing energy calculated by including (full symbols) or not (empty symbols) the interaction with Al and F core states. (a) Al<sub>2</sub>F<sub>3</sub> clusterlike surface (circles); (b) Al<sub>2</sub>F<sub>3</sub> clusterlike surface (squares).

ion fraction  $\Gamma^{\text{ion}} = \Gamma^- + \Gamma^+$ , are shown as a function of the outgoing energy. The calculation describes correctly the general dependence with energy, being approximately 10% above the experiment. An important positive ion fraction (an average value of  $\Gamma^+ \sim 45\%$ ) and a small negative fraction  $\Gamma^- \sim 5\%$  were obtained. Figure 4(b) shows the results for hydrogen going out from the initial position (B) [Fig. 1(b)], which involves the AlF<sub>3</sub> clusterlike surface of Fig. 2(b). In this case the calculation describes the predominance of the positive ion fraction, however it does not reproduce the general behavior with outgoing energy. By taking into account that the probability for the initial position (A) is twice the one for (B) (because of the F to Al atom ratio at the surface), an average of the two cases was performed. This averaged result shows a better agreement with the experiment, as it is observed in Fig. 5. These all calculations were also performed by assuming a neutral initial state configuration, and in this case the results did not reproduce the experimental trends. Then for a ionic surface the initial charge state condition becomes important, being the positive ion the more appropriate one.

The contributions  $|G_{aM}(t, t_0)|^2$  of the different MO states ( $\Phi_M$ ) of the surface to the neutralization of H<sup>+</sup> [Eq. (7)] are shown in Fig. 6(a) for the case of the Al<sub>2</sub>F<sub>3</sub> clusterlike surface. The MO states that contribute mostly in this case are indicated as  $\Phi_{14}$ ,  $\Phi_{18}$ ,  $\Phi_{19}$ , and  $\Phi_{20}$ . The MO  $\Phi_{14}$  is essentially a 2s atomic orbital of the F atom lying between two Al atoms (the nearest to the hydrogen projectile in its initial

position), and  $\Phi_{19}$  is essentially a  $2p_z$  of the same F atom.  $\Phi_{18}$  and  $\Phi_{20}$  are combinations of  $2p_z$  and  $2p_y$  atomic orbitals of the three F atoms of the cluster. From Fig. 6(a) one can conclude that the interaction between hydrogen and the nearest F atom is dominating the neutralization at low and large outgoing energies, while at intermediate (around 1.5 keV) and very low (0.5 keV) energies all the F atoms contribute. The contributions of MO indicated as  $\Phi_9, \Phi_{12}, \Phi_{14}, \Phi_{15}, \Phi_{16}$  to the hydrogen charge in the case of AlF<sub>3</sub> clusterlike surface are shown in Fig. 6(b). For energies lower than 1 keV the main contribution comes from F atoms at the surface ( $\Phi_{12}$  and  $\Phi_{15}$  are combinations of  $2p$  atomic orbitals centered on the surface F atoms), while for larger energies the interaction with all F atoms determines the neutralization of hydrogen ( $\Phi_{14}$  and  $\Phi_{16}$  are combinations of  $2p$  atomic orbitals of the three F atoms, while  $\Phi_9$  results from the combination of F-2s). Similar contributions of all these MO states were found for the lowest energy value considered (0.5 keV). Although the charge exchange takes place mainly between the hydrogen and the valence band states of the surface, the strong interaction with the core states of target atoms can either promote or inhibit this process. Figure 7 shows the positive ion fraction obtained by omitting the core states in the calculation. In both clusterlike surfaces it is observed that the interaction with the core states (F-1s, F-2s, and Al-2s) decreases the probability for electron capture from the valence band in practically all the analyzed energy range. The role of the core states is more important in the case of the Al<sub>2</sub>F<sub>3</sub> surface where the close interaction with the nearest F atom defines the hydrogen state occupation. This occupation along the outgoing trajectory is shown in Fig. 8 for the Al<sub>2</sub>F<sub>3</sub> clusterlike surface; the full calculation is compared with the one that omits the core states for two different outgoing energies (0.75 and 3 keV). Large oscillations due to quantum interference phenomena along the outgoing trajectory are observed for distances close to the surface, being more pronounced for lower energies. This oscillation pattern is strongly altered when considering or not the core states, leading in each case to different final values for the occupation. This effect is mainly due to the effective ion energy level defined by the hybridizations with the inner states. Accordingly with this analysis, the charge transfer process in the case of hydrogen going out from AlF<sub>3</sub> surface occurs mainly for close distances involving the nearest surface atoms. The Al<sub>2</sub>F<sub>3</sub> clusterlike surface is expected to represent a more realistic situation for the emission process, because it is more favorable for H<sup>+</sup> to leave the surface nearer to a F<sup>-</sup> than to an Al<sup>2+</sup>.

#### IV. CONCLUSIONS

In the large incoming energy range and large scattering angle situation studied in this work the outgoing trajectory of the projectile is crucial to define its final charge state. The initial charge configuration for the emission process is acquired along the crossing of the surface layer, and it depends strongly on the characteristics of the band structure of the surface. The effective and total neutralization occurring in the case of a wide band metallic surface is largely inhibited

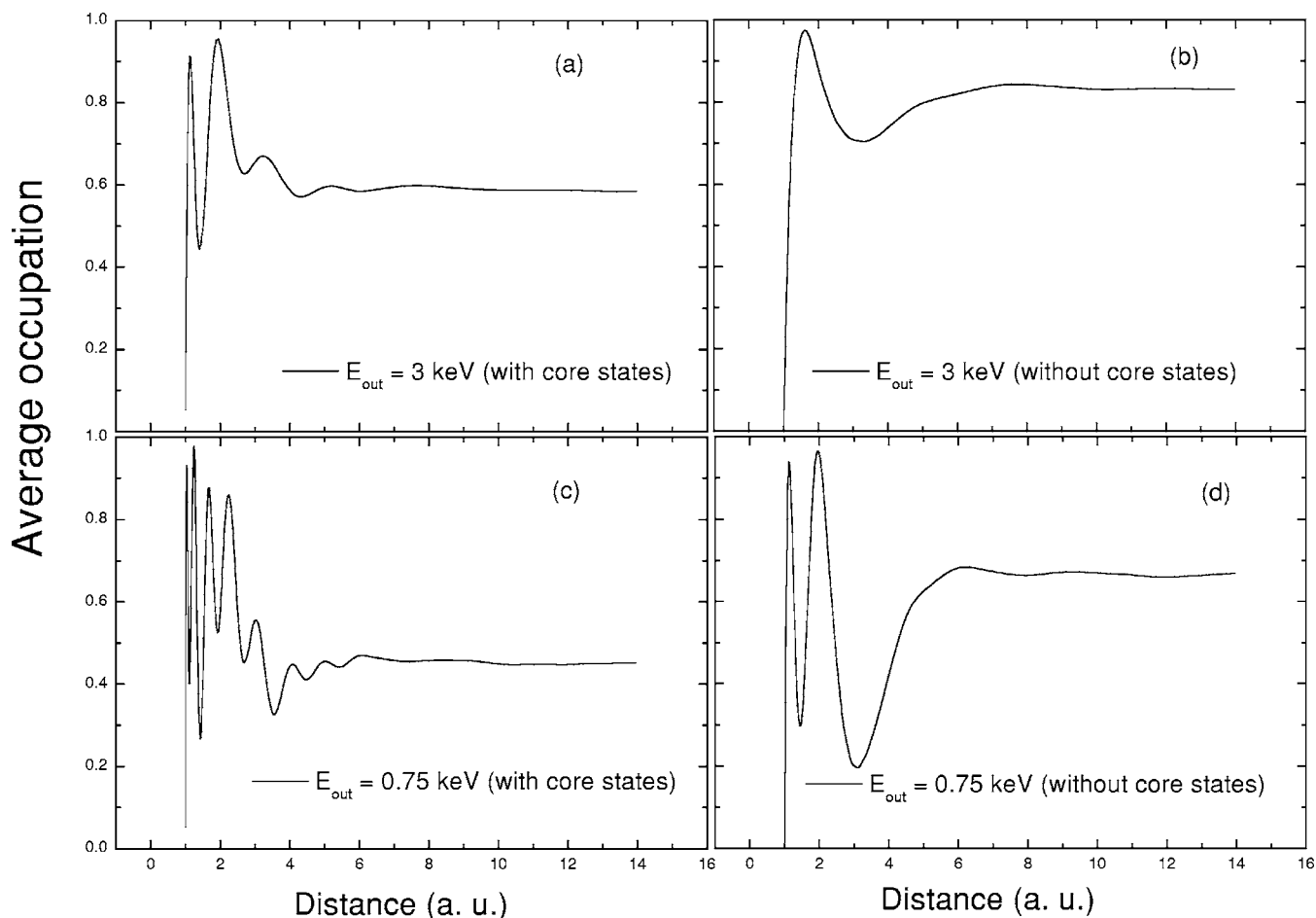


FIG. 8. Hydrogen state occupation as a function of the distance from the surface calculated with (a and c) and without (b and d) the contribution of F and Al core states for the  $\text{Al}_2\text{F}_3$  clusterlike surface and for outgoing energy values: 3 and 0.75 keV, respectively.

in ionic surfaces of relatively narrow band and large band gap. Thus the negative ion formation is more probable in the case of metallic surfaces like Al than in the ionic surfaces like  $\text{AlF}_3$ , being expected in the last case a significant positive ion fraction. Consistently, the same results were obtained by considering either a neutral or a negative charge state as initial conditions for the emission from a pure Al surface, while in the emission from  $\text{AlF}_3$  the positive charge state was the only one that provided a good description of the experimental results. Our calculation takes into account the short-range interactions and the level shift of the projectile due to either image or Madelung potentials. It is found that in the Al surface case the strong hybridizations occurring in the close distance region do not affect the hydrogen final charge state, while in  $\text{AlF}_3$  the interaction with the core states are inhibit-

ing the neutralization for practically all the outgoing energy range analyzed. Then it is concluded that the close encounter is more important to define the final charge state of hydrogen going out from  $\text{AlF}_3$  than from a clean Al surface.

#### ACKNOWLEDGMENTS

This work was supported by Grants (PIP) No. 0 2833/99 from Consejo Nacional de Investigaciones Científicas y Tecnológicas (CONICET), (CAI+D) No. 6-1-76 from Universidad Nacional del Litoral (UNL), Argentina. We acknowledge partial financial support from the ANPCyT (PICTs 03-03579/06249/6325/14452), CONICET (PIP 0423), and Fundación Antorchas (A-13927-17, 14022/111).

\*Fellow of Agencia Nacional de Promoción Científica y Tecnológica ANPCyT.

<sup>1</sup>R. S. Bhattacharya, W. Eckstein, and H. Verbeek, *Surf. Sci.* **93**, 563 (1980).

<sup>2</sup>H. Verbeek, W. Eckstein, and R. S. Bhattacharya, *Surf. Sci.* **95**,

380 (1980).

<sup>3</sup>R. Souda, K. Yamamoto, W. Hayami, T. Aizawa, and Y. Ishizawa, *Phys. Rev. B* **51**, 4463 (1995).

<sup>4</sup>R. Souda, T. Suzuki, and K. Yamamoto, *Surf. Sci.* **397**, 63 (1998).



- <sup>5</sup>M. Casagrande, S. Lacombe, L. Guillemot, and V. A. Esaulov, *Surf. Sci.* **445**, L29 (2000).
- <sup>6</sup>M. Maazouz, R. Baragiola, A. Borisov, V. A. Esaulov, J. P. Gauyacq, L. Guillemot, S. Lacombe, and D. Teillet-Billy, *Surf. Sci.* **364**, L568 (1996).
- <sup>7</sup>M. Maazouz, A. Borisov, V. A. Esaulov, J. P. Gauyacq, L. Guillemot, S. Lacombe, and D. Teillet-Billy, *Phys. Rev. B* **55**, 13869 (1997).
- <sup>8</sup>M. Maazouz, L. Guillemot, S. Lacombe, and V. A. Esaulov, *Phys. Rev. Lett.* **77**, 4265 (1996).
- <sup>9</sup>M. Maazouz, S. Ustaze, L. Guillemot, and V. A. Esaulov, *Surf. Sci.* **409**, 189 (1998).
- <sup>10</sup>S. Ustaze, R. Verucchi, S. Lacombe, L. Guillemot, and V. A. Esaulov, *Phys. Rev. Lett.* **79**, 3526 (1997).
- <sup>11</sup>A. G. Borisov and V. A. Esaulov, *J. Phys.: Condens. Matter* **12**, R177 (2000).
- <sup>12</sup>J. Los and J. J. C. Geerlings, *Phys. Rep.* **190**, 133 (1990).
- <sup>13</sup>M. C. Torralba, P. G. Bolcatto, and E. C. Goldberg *Phys. Rev. B* **68**, 075406 (2003).
- <sup>14</sup>V. A. Esaulov, S. Ustaze, M. Maazouz, L. Guillemot, and R. Verucchi, *Surf. Sci.* **380**, L521 (1997).
- <sup>15</sup>Evelina A. García, P. G. Bolcatto, M. C. G. Passeggi, and E. C. Goldberg, *Phys. Rev. B* **59**, 13370 (1999).
- <sup>16</sup>J. O. Lugo, E. C. Goldberg, E. A. Sánchez, and O. Grizzi, *Phys. Status Solidi A* **201**, 2356 (2004).
- <sup>17</sup>J. O. Lugo, E. C. Goldberg, E. A. Sánchez, and O. Grizzi, *Phys. Rev. B* **72**, 035432 (2005).
- <sup>18</sup>F. Guinea, C. Tejedor, F. Flores, and E. Louis, *Phys. Rev. B* **28**, 4397 (1983).
- <sup>19</sup>P. G. Bolcatto, E. C. Goldberg, and M. C. G. Passeggi, *Phys. Rev. B* **58**, 5007 (1998).
- <sup>20</sup>E. C. Goldberg, E. R. Gagliano, and M. C. G. Passeggi, *Phys. Rev. B* **32**, 4375 (1985).
- <sup>21</sup>L. V. Keldysh, *Zh. Eksp. Teor. Fiz.* **47**, 1515 (1964) [*Sov. Phys. JETP* **20**, 1018 (1965)].
- <sup>22</sup>Ph. Daniel, A. Bulou, M. Rousseau, J. Nouet, J. L. Fourquet, M. Leblanc, and R. Burriel, *J. Phys.: Condens. Matter* **2**, 5663 (1990).
- <sup>23</sup>This calculation was performed using the commercial program GAUSSIAN98 (Gaussian, Inc., Pittsburgh, 1998).
- <sup>24</sup>P. G. Bolcatto, E. C. Goldberg, and M. C. G. Passeggi, *Phys. Rev. A* **50**, 4643 (1994).
- <sup>25</sup>J. O. Lugo, L. I. Vergara, P. G. Bolcatto, and E. C. Goldberg, *Phys. Rev. A* **65**, 022503 (2002).